Synthesis of Supramolecular Polymers by Ionic Self-Assembly of Oppositely Charged Dyes

Ying Guan,[a] Shu-Hong Yu,[a, d] Markus Antonietti,[a] Christoph Böttcher,[b] and Charl F. J. Faul*[a, c]

Abstract: A new type of supramolecular polymer was prepared by ionic self-assembly (ISA) from two oppositely charged dyes; a perylenediimide and a copper–phthalocyanine derivative. Coulomb coupling stabilizes the whole structure, and a combination of charge-transfer interactions and discotic stacking facilitates the exclusive formation of one-dimensional polymeric chains. The supramolecular dye-polymers have a large association constant (2.4× $10^7 \, L \, mol^{-1}$), high molecular weight, and high mechanical stability. The use of cryo-transmission electron microscopy (cryo-TEM) confirmed the existence of extended fibers of width 2.4 nm. Further image analysis revealed slight undulation and faint segmenta-

tion of the fibers, and density maxima were observed at a regular interval of 3.6 nm along the fiber axis. The fiber-like structure (and aggregate of fibers) is also found in the solid state, as shown by the results of mineralization contrasting experiments, atomic force microscopy (AFM), and X-ray analyses. A structural model is proposed, in which the structural subunits, arranged in a side-by-side conformation, form a stacked structure.

Introduction

The wide range of properties exhibited by supramolecular polymers, such as the facile inclusion of functional mono-

[a] Dr. Y. Guan, Prof. Dr. S.-H. Yu, Prof. Dr. M. Antonietti, Dr. C. F. J. Faul
Max Planck Institute of Colloids and Interfaces
Research Campus Golm, 14424 Potsdam (Germany)
Fax: (+49) 331-567-9502
E-mail: charl.faul@mpikg-golm.mpg.de

[b] Dr. C. Böttcher
Forschungzentrum für Elektronenmikroskopie
Freie Universität Berlin, Fabeckstrasse 36a, 14195 Berlin (Germany)

[c] Dr. C. F. J. Faul
New Address:
University of Bristol, School of Chemistry
Inorganic and Materials Chemistry, Bristol, BS8 1TS (UK)
E-mail: charl.faul@bristol.ac.uk

[d] Prof. Dr. S.-H. Yu
Current Address:
Division of Nanomaterials and Chemistry
Hefei National Laboratory for Physical Sciences at Microscale
Department of Materials Science and Engineering
University of Science and Technology of China
Hefei 230026 (P. R. China)

Supporting information for this article is available on the WWW under http://www.chemeurj.org/ or from the author: UV/Vis spectra of the PTDI-1/CuPcTS complex in different concentrations and films.

mers and their intricate, supramolecular structure, has stimulated recent interest in these systems.[1] Comparison of supramolecular polymers with common polymers shows that they exhibit reversible binding/aggregation behavior, that is, they can dissociate and recombine within experimental time scales. This implies that they can, for instance, undergo self-repair following fracture and can adapt their viscoelastic behavior towards external stimuli in a way that is not possible for traditional macromolecules. The combination of properties of supramolecular polymers assigns them to a unique class of novel materials.

Until now, the synthesis of supramolecular polymers has involved highly directional, noncovalent interactions, such as hydrogen bonding,[2] metal coordination,[3] and arene–arene interactions[4] (based on discotic molecules with a disc-shaped core and a number of peripheral, flexible side-chains), to ensure a predominantly linear character. Another prerequisite is that the association constant for the repeating units should be large enough to give polymers with a high molecular weight. This has been achieved through a combination of secondary interactions.[5]

On the other hand, ionic self-assembly[6] (ISA), that is, self-organization on the basis of electrostatic interactions, has proved to be a powerful tool for the creation of new nanostructures and chemical species.[7] Because electrostatic interactions between charged species are, in principle, non-

directional, ISA has not, until now, been employed for the synthesis of supramolecular polymers. The strong interactions mediated by multiple electrostatic bonds may, however, result in large association constants, provided that secondary aggregation of the ion pairs (due to dipole and multipole interactions) can be kept strictly intramolecular by the appropriate architecture of the charged tectons. This implies that supramolecular polymers can be designed by combining highly directional, noncovalent tecton interactions with electrostatic coupling.

To test this approach, two extended dye systems, a cationic perylenediimide (PTDI-1,[8] two charges) and a negative copper–phthalocyanine tetrasulfonate (CuPcTS, four charges) were chosen as monomeric units to form a supramolecular polymer.

These two tectons were chosen on the basis of their func-

PTDI-1

CuPcTS
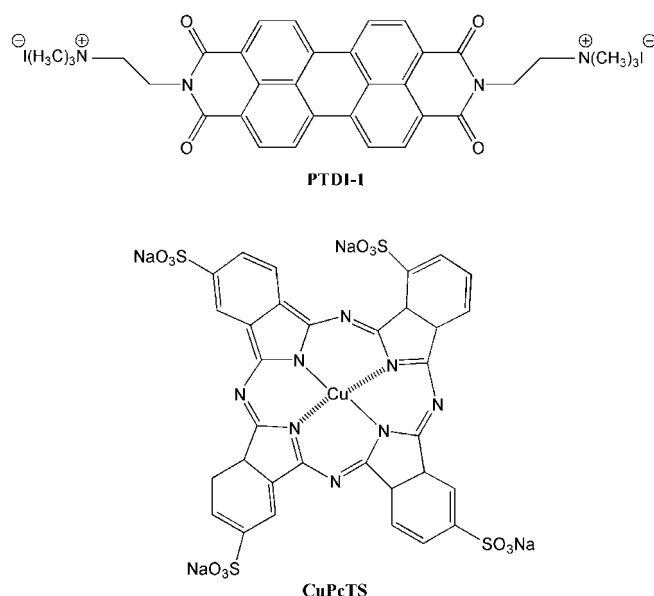
tion, as well as for purely geometric reasons. Perylenediimide derivatives and phthalocyanine or porphyrin derivatives have attracted much attention through their use as electrophotographic photoreceptors, photovoltaic elements, as well as for the storage of optical data.[9] Amongst these compounds, perylene–porphyrin building blocks[10] and linear arrays of perylene, porphyrin, and phthalocyanine units[11] have been designed and synthesized by means of covalent reactions, with the aim that the resulting superstructures might simultaneously provide two independent pathways for electron and hole conduction. The application of perylene and phthalocyanine double-layer or multilayer devices[12] in solar cells[13] has also been reported. It is expected that an appropriately designed supramolecular polymer of perylene and phthalocyanine derivatives will have similar applications, but with the advantages of being simple to synthesize and, in the absence of covalent constraints, being able to adopt an optimal structure.

Results and Discussion

The interaction between PTDI-1 and CuPcTS in water was studied by using UV/Vis and fluorescence spectroscopy. Figure 1 shows the UV/Vis titration spectra. The absorbance
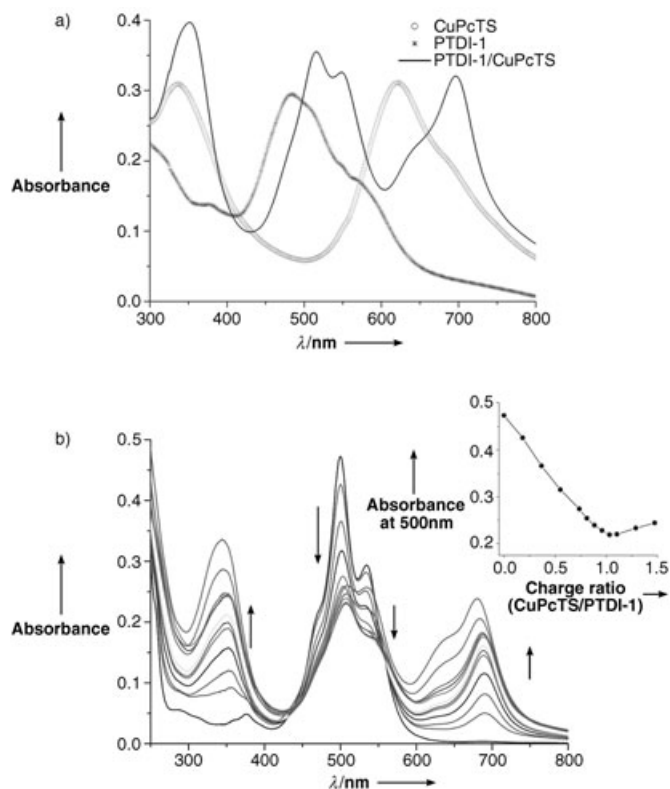

Figure 1. a) UV/Vis spectra of pure dyes and complex films cast from aqueous solution. b) UV titration experiment of PTDI-1 (10^{-5} M in water) with CuPcTS; inset: absorbance at 500 nm as a function of CuPcTS concentration.

of the S_0–S_1 electronic transition of perylene at 500 nm decreases as the content of CuPcTS increases, whereas the intensities of the B-band (at 351 nm) and Q-band (at 689 nm) of CuPcTS increase. An isosbestic point at 556 nm appears before, and disappears after, the charge-equivalent point of PTDI-1 and CuPcTS. This observation indicates that a 1:1 charge ratio complex of PTDI-1 and CuPcTS forms in the solution.

The inset of Figure 1b shows the absorbance at 500 nm as a function of CuPcTS concentration. The absorbance at 500 nm clearly decreases linearly as the concentration of CuPcTS increases, and then increases after the charge-equivalent point, at a charge ratio of 1.04. Deviations from the value of one may be due to the presence of minor impurities within the starting products and will be discussed below. The results indicate that the PTDI-1/CuPcTS complex forms quantitatively in solution, even at the very low concentrations used for UV/Vis spectroscopy.

In comparison with pure dyes, all of the absorption peaks of the PTDI-1/CuPcTS complex show a red shift. The red shift of the complex spectrum is more pronounced in the solid state (see Figure 1a); 17.2 nm for the B-band absorption of CuPcTS, 38.7 nm for the perylene absorption maximum of the S_0–S_1 electronic transition, and 83.7 nm for the Q-band absorption of CuPcTS. The changes in the UV/Vis spectrum are the result of the desired electronic coupling or charge-transfer interactions between the two components.

PTDI-1 exhibits strong green fluorescence with a maximum intensity at 545.5 nm when excited at 480 nm. Figure 2
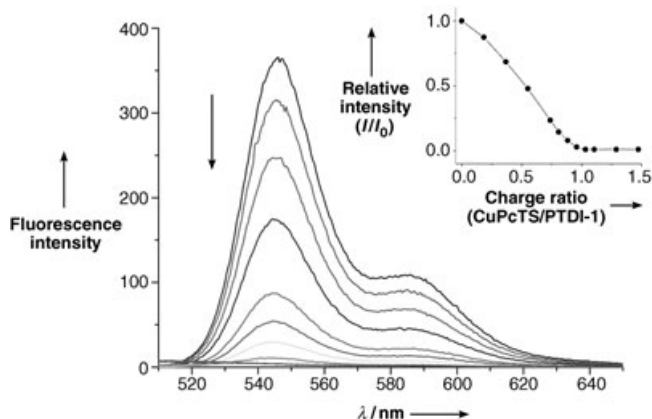

Figure 2. Fluorescence titration of PTDI-1 (10^{-5} M in water, $\lambda_{exc}=485$ nm) with CuPcTS; inset: relative fluorescence intensity (I/I_0) at 545.5 nm following addition of CuPcTS.

shows that the fluorescence of PTDI-1 can be completely quenched by the addition of CuPcTS. The fluorescence intensity decreases in an almost linear fashion as the concentration of CuPcTS is increased (inset of Figure 2); however, the wavelength that exhibits maximum fluorescence changes very little. The PTDI-1 fluorescence is quenched completely at the charge-equivalence point.

This again indicates the formation of a very well-defined PTDI-1/CuPcTS complex, in which the perylene and phthalocyanine molecules have a strict geometric association with each other (or else quenching would be more efficient and not only observed at the exact stoichiometric balance).

These results show that it is possible to construct a supramolecular polymer of high molecular weight at higher concentrations. However, it is still unclear whether this polymer would be linear and structurally well-defined, or gel-like, as the reaction of a four-functional cross-linker with a two-functional monomer can, in principle, lead to the formation of extended gels. During the addition process, a significant increase in viscosity was observed (provided the initial "polymerization" between PTDI-1 and CuPcTS occurred in solution), and reached a maximum at the charge-equivalent point of PTDI-1 and CuPcTS. This increase in viscosity is a typical property of supramolecular polymers.[14]

The CuPcTS/PTDI-1 complex was precipitated from ethanol to remove salts and then dried under vacuum. The precise 1:1 charge ratio was verified by performing elemental analysis, in which the absence of sodium and bromide counterions was confirmed. This result supports the interpretation that the deviations from the exact stoichiometry that were recorded in the phototitration experiments were presumably due to impurities. The complex was then redissolved in water to enable analysis of the supramolecular polymer structure. It must be emphasized that in pure, deionized water and in the absence of small ions, the formation of the self-assembled structure is practically irreversible.

The UV/Vis spectra reveal the concentration-dependent aggregation of primary elements to form the primary superstructures, for concentrations $<10^{-4}$ mg mL^{-1} (see Supporting Information). This aggregation process may occur in two steps: Firstly, a basic unit at a charge ratio of 1:1, namely, (PTDI-1)$_2$(CuPcTS), is formed. This step is quantitative and irreversible. These basic units aggregate to form superstructures with an association constant of 2.4×10^7 L mol^{-1}, which was calculated based on an equal-K model according to reference [15]. The large association constant is clearly due to the combination of electronic interactions between the dyes, the potential discotic packing, and, as a driver, the electrostatic interactions between CuPcTS and PTDI-1.

As shown in Figure 3, the viscosity of the solution increases dramatically as the concentration increases. A solution with a concentration of 4.0 mg mL^{-1} has a viscosity approxi-
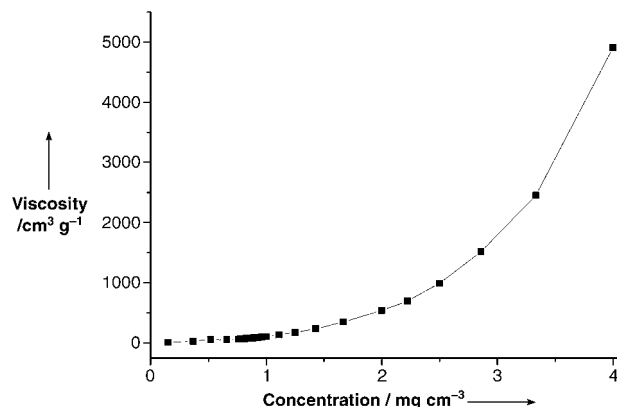

Figure 3. Effect of concentration of the PTDI-1/CuPcTS polymer on viscosity.

mately 900 times higher than that of a solution of 1.5×10^{-1} mg mL^{-1}. The high viscosity at such low concentrations indicates that rod-like, high molecular weight, supramolecular polymers form in solution, and the concentration-dependent change in molecular weight is characteristic for supramolecular polymers. This phenomenon is very similar to the behavior of so-called organogelators.[16]

Cryo-transmission electron microscopy (cryo-TEM) was used to investigate the extended supramolecular structure. Figure 4 shows results of the direct imaging of a 1.68 mg mL^{-1} solution of the complex, in which long fibers
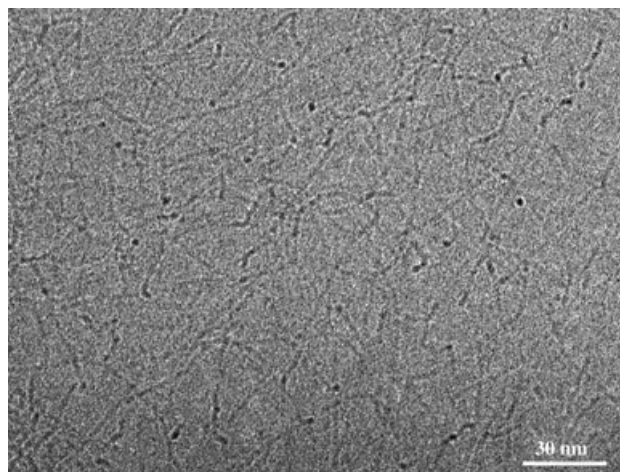
Figure 4. Cryo-TEM image of a polymer solution at a concentration of 1.68 mg mL^{-1}.

are visible. From the number of fibers and the number of ends seen, we can estimate the length of the fibers to be in the μm range. The fibers have an average thickness of 2.4 nm, determined by analysis of digitally extracted and aligned single-fiber motifs (see Supporting Information). Interestingly, the fiber ends are visible as dark points in the TEM image. This is similar to the ends of the supramolecular fiber formed from pseudoisocyanine dyes.[17]

Because a vague, internal structure could be detected from the highly resolved micrographs of the single-fiber motif, further single-particle analysis of approximately 1000 fiber segments, digitally extracted from three micrographs, was performed. The individual motifs were aligned, analyzed by multivariate statistics, classified, and cummulated to give a set of class sum images, which represent structural differences in the data set. Each class sum image was obtained from the sum of several (15–25) individual images containing identical information. Therefore, the signal-to-noise ratio was improved by averaging out any random information. This procedure is well established for the analysis of natural as well as synthetic supramolecular architectures and has been used routinely for the three-dimensional reconstruction of, for example, protein structures[18,19] or structurally persistent, supramolecular assemblies.[20,21]

Figure 5 (top image) shows the 11 most statistically significant class averages. The diameter in all images is almost identical; however, the most striking difference is a slight undulation (e.g., location 11) and a faint segmentation along the fiber axis. The latter can be visualized more clearly by combining 194 individual images of aligned fibers in a single class at the expense of a slight increase in data variance (Figure 5, bottom image). The result of this summation clearly indicates a regularly repeating density maximum with a periodicity of about 3.6 nm. Although it cannot be proven conclusively, the repeating density maxima, seen in conjunction with the undulations and segmentation of the fibers, could suggest a helical arrangement of the dye subunits (see also Scheme 1).
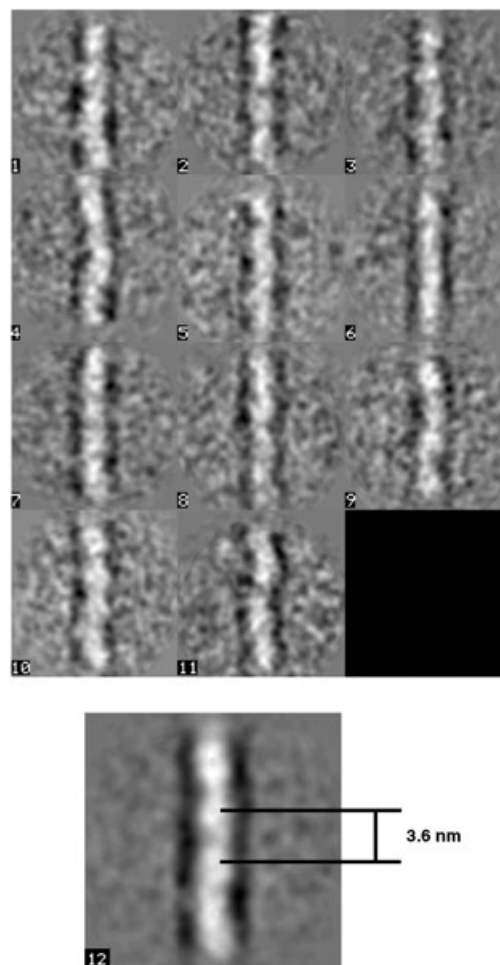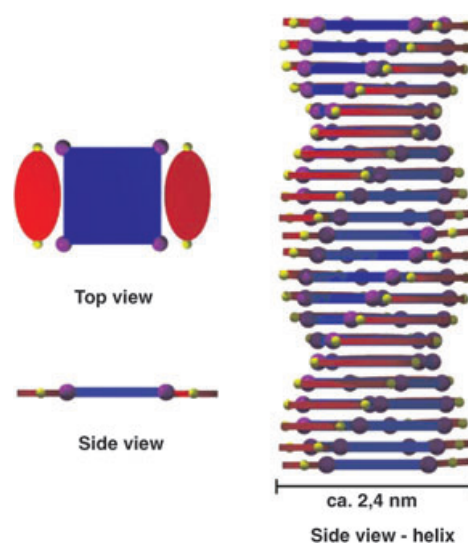

Figure 5. Locations 1–11 show the statistically most significant class averages out of ~1000 individual fiber segments. Each class contains 15–20 individual images aligned. Location 12 represents the total sum of 194 aligned images, revealing the repeating density maxima with a better signal-to-noise ratio.

Scheme 1. Proposed arrangement of the dye tectons into a helical, fiber-like structure.

To confirm the formation of rod-like, polymer chains in solution, marker/contrasting experiments[22] using both CdS nanoparticles and $CaCO_3$ mineralization were performed. SEM and TEM examination revealed fibrous structures throughout the whole sample, as shown in Figure 6.

The successful adherence of nanoparticles is due to the presence of charge pairs within the supramolecular polymers, which causes accumulation of inorganic ions at the polymer surface. The $CaCO_3$ contrasting experiments reveal large bundles of fiber-like aggregates micrometers in length (Figure 6a). CdS contrasting experiments enable the visualization of contrasted polymer strands down to around 3 nm in width (due to

Direct examination of the high concentration phase or solid (PTDI-1)$_2$CuPcTS complex by using atomic force microscopy (AFM) also revealed a fiber-like structure (Figure 7), indicating that the complex maintains its supramolecular aggregation motif even in the pristine solid state.
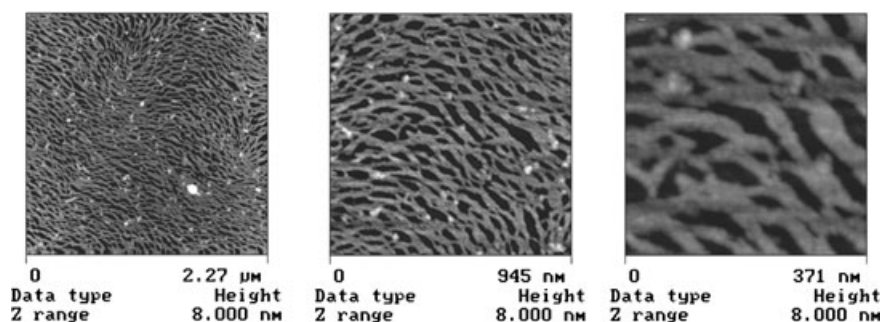

Figure 7. AFM images of the (PTDI-1)$_2$CuPcTS complex (10 µL of 0.125 mg mL^{-1} solution of PTDI-1/CuPcTS on mica).
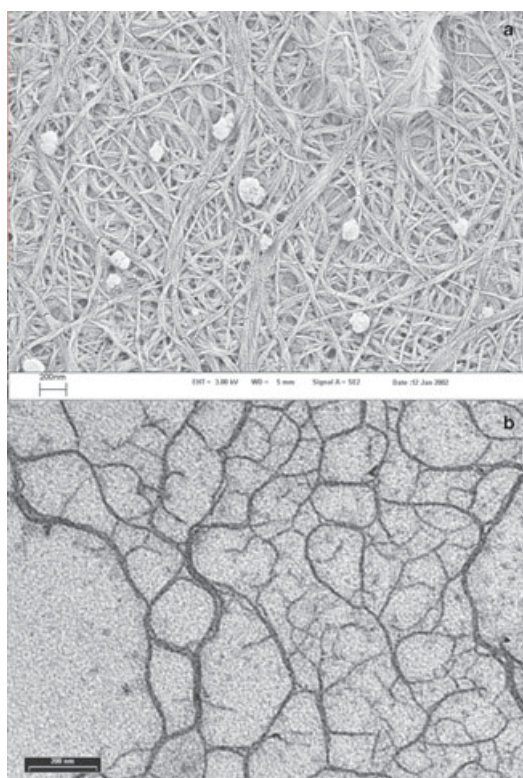

Figure 6. a) SEM image (fixation with $CaCO_3$) and b) TEM image (CdS contrasted) of the PTDI-1/CuPcTS polymer. Structural changes due to fixation/contrasting cannot be excluded. Each scale bar represents a distance of 200 nm.

the coating of a very thin layer of nanoparticles around the rod-like polymer structures). Aggregation of these 3 nm rod-like structures was confirmed by the presence of superaggregates of widths 6–9, 12–15, and 18–20 nm, respectively (Figure 6b).

The average thickness of the fiber strands is approximately 20–25 nm, with an average height of approximately 2.5 nm. These strands are clearly lateral superaggregates of several single fibers, with the height of a single polymer (measured by using cryo-TEM). Such lateral aggregation is typical for fiber-like aggregates and is also well-known for organogelators. The self-assembly of single, supramolecular fibers into strands and fiber bundles is presumably driven by entropic interactions (typical for stiff polymer chains[23]), with additional support from multipolar (i.e., dipolar and quadrupolar) interactions between the single, supramolecular polymer chains.

The X-ray scattering intensities of solutions of the polymer were too low to be analyzed by using lab-based X-ray techniques; due to the extremely high viscosity, samples of concentrations greater than 11 mg mL^{-1} could not be prepared. Therefore, powder X-ray diffraction analyses in the pristine solid state were performed to reveal further details of the structure of the polymeric (PTDI-1)$_2$CuPcTS complex. Results of small-angle X-ray scattering (SAXS) analyses at room temperature (Figure 8a) revealed two reflections at d-spacings of 1.71 nm and 0.62 nm, which are maintained even after heating the solid material to 200°C and re-cooling to room temperature. Broad and weak reflections were also observed (marked by arrows in Figure 8a), which correspond to approximate distances of 7.6 nm and 1.0 nm, respectively. A plot of $\log I$ versus $\log q$ produced a gradient of -1, which fitted very well with a Kratky–Porod, worm-like chain structure model (see Supporting Information), and supports further the assumption that the solid state is composed of well-aligned, supramolecular fibers.

Wide-angle X-ray scattering (WAXS) analyses (Figure 8b, partly overlapping the region analyzed by using SAXS) revealed a peak corresponding to 0.33 nm (in addition to the peak at 0.62 nm, which was also seen in the SAXS diffractogram). This reflection at 0.33 nm corresponds to the typical
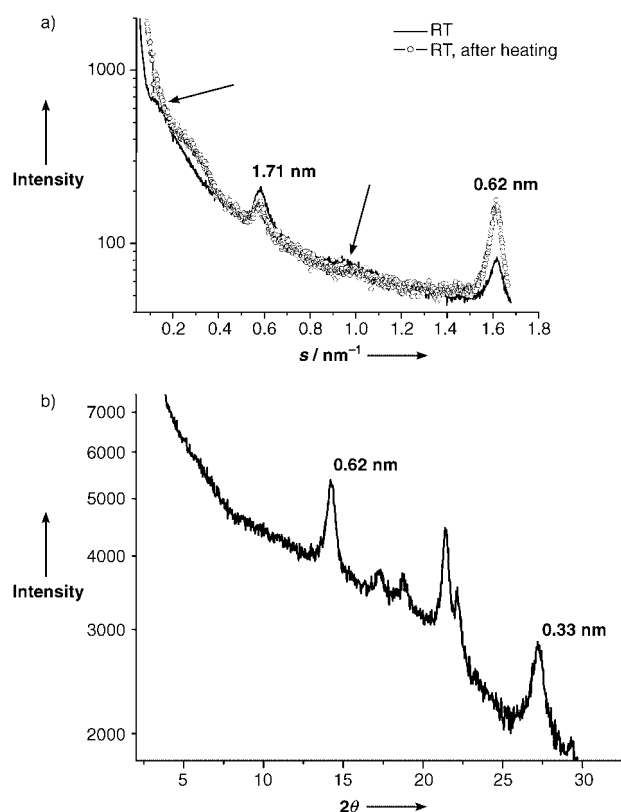
Figure 8. Small-angle (a) and wide-angle (b) X-ray scattering analyses of the PTDI-1/CuPcTS polymer in the solid state.

discotic stacking distance of aromatic systems, such as perylene and/or phthalocyanine cores.

The peak at 1.71 nm was tentatively assigned to the distance between single fibers within the aligned domains. The smaller distance, relative to that in aqueous solution (measured by using cryo-TEM), may well be due to the dehydration and consecutive compaction/lateral intercalation between fibers. Helicity along the fiber axis would assist in this packing arrangement, and could explain the reflection at 0.62 nm as an in-plane packing motif (see Scheme 1). In any case, the strong peak at 0.33 nm proves that the whole structure is composed of dye stacks.

Based on these observations, we tentatively propose a structural model of the supramolecular polymer. Because the maximum molecular extensions of the PTDI-1 and CuPcTS are calculated to be approximately 1.48 nm[24a] and 1.2 nm,[24b] respectively, the fibers (with a thickness of 2.4 nm and a molar ratio of 2:1 to satisfy the requirement of charge neutrality) are presumably triple stacks, as depicted in Scheme 1.

The potential helicity of this model would be a direct consequence of packing, as would the dipolar interactions between single ion pairs, as every ion can also preferentially interact with the oppositely charged ion in the next layer. Therefore, this structure not only satisfies charge neutrality, but may also explain the fiber thickness of 2.4 nm, the regu-

lar density maxima, the slight undulation, and the faint segmentation along the fibers.

This model also supports the UV and fluorescence data, because the proposed side-by-side arrangement ensures close proximity and maximal electronic coupling of the dyes by aligning tendencies to polarize and transition moments in parallel. The proposed model reasonably and simply accounts for all of the observations made by spectroscopy, TEM, and X-ray analysis. Nevertheless, more complicated packing arrangements cannot be excluded.

Conclusion

A strategy that makes use of the ionic self-assembly principle for the production of a new class of supramolecular polymers is presented. The polymers were prepared by the simple addition of two oppositely charged dyes; a perylene-diimide and a copper–phthalocyanine derivative. A combination of charge-transfer interactions and discotic stacking facilitates the formation of one-dimensional chains, and electrostatic Coulomb coupling stabilizes the whole structure so that the dyes form polymeric stacks of high molecular weight and mechanical stability. This was confirmed in solution as well as in the solid state by using a variety of direct and indirect imaging techniques. Image analysis of the TEM data showed slight undulation and faint segmentation of the fibers, and a density maximum at a regular interval of 3.6 nm along the fiber axis, which suggests the formation of a regular, helical structure. A helically twisted, triple stack model was proposed, which correlates well with the structural and spectroscopic observations.

Appropriately designed polymers of a similar type have potential for various applications, such as electro-optic devices as well as for light-harvesting. In addition, with their highly regular and dipolar exterior, they are promising as nucleating mineralization templates, as exemplified by the use of $CaCO_3$ and CdS.

Experimental Section

Materials: PTDI-1 was synthesized and purified according to a published procedure.[8] CuPcTS was obtained from Sigma-Aldrich, and used as received. All complexations (slow addition of CuPcTs to PTDI-1 until a 1:1 charge ratio was reached) were performed in pure, deionized water.

Instruments: UV/Vis spectra were recorded by using a Perkin–Elmer Lambda 2 spectrometer. Steady-state fluorescence spectra were recorded by using a Perkin–Elmer LS50B luminescence spectrometer. Emission spectra were recorded in the range of 400 to 800 nm by using an excitation wavelength $\lambda_{exc} = 480$ nm. Both the excitation and emission band-widths were 2.5 nm. All viscosity measurements were performed by using a standard capillary viscometry apparatus (Lauda S5 Automated Viscometer, Schott temperature-controlled water bath) at 25°C. Elemental analyses (C, H, N, S) were performed by using a Vario EL Elementar (Elementar Analysensysteme, Hanau, Germany).

Electron cryomicroscopy preparation: Droplets of the sample (5 μl) were applied to perforated (hole diameter 1 μm) carbon-film-covered 200 mesh grids (R1/4 batch of Quantifoil Micro Tools GmbH, Jena, Ger-

many), which had been hydrophilized before use by performing plasma treatment for 60 s at 8 W in a BALTEC MED 020 device. The supernatant fluid was removed by using filter paper to leave an ultrathin layer of the sample solution, which spanned the holes of the carbon film. The samples were immediately vitrified by dropping the grids into liquid ethane at its freezing point (90 K) and by operating a guillotine-like plunging device. The vitrified samples were subsequently transferred under liquid nitrogen into a Philips CM12 transmission electron microscope (FEI Company, Oregon, USA) by using the Gatan (Gatan Inc., California, USA) cryoholder and stage (Model 626). Microscopy was performed at a sample temperature of 94 K by using the low-dose protocol of the microscope at a primary magnification of $\times 58\,300$ and with an accelerating voltage of 100 kV (LaB_6-illumination). In all cases, the defocus was set to 0.9 μm, which corresponds to a first zero of the phase-contrast transfer function at 1.8 nm.

Image processing: Prior to processing, micrographs were checked for the absence of astigmatism or drift by using laser optical diffraction. Optical sound micrographs were digitized by using the Heidelberg "Primescan" drum scanner (Heidelberger Druckmaschinen AG, Heidelberg, Germany) at a nominal pixel resolution of 1.81 Å in the digitized images (scanning resolution 1 μm). A total of 983 individual fiber segments were selected and extracted from three digitized micrographs as 100×100 pixel fields. After suppressing high frequency background noise by means of filtering, well-established "reference-free" alignment and classification procedures[25] were performed by using multivariate statistical analysis and hierarchical classification schemes, with the aid of IMAGIC-5 software (Image Science GmbH, Berlin, Germany). Structural differences in the data yielded a set of "class averages", each representing a "typical view" of a noise-reduced, two-dimensional projection image. Twelve of the 100 statistically significant classes (lowest intraclass variance) are represented in Figure 5.

Small-angle X-ray scattering (SAXS) measurements were performed by using a Nonius rotating anode ($U = 40$ kV, $I = 100$ mA, $\lambda = 0.154$ nm) and image plates. With the image plates placed at a distance of 40 cm from the sample, a scattering vector range of $s = 0.07$–1.6 nm^{-1} was available. Two-dimensional diffraction patterns were transformed into one-dimensional radial averages. The data noise was calculated according to Poisson statistics, which are valid for scattering experiments.

Wide-angle X-ray scattering (WAXS) measurements were performed by using a Nonius PDS120 powder diffractometer in transmission geometry mode. An FR590 generator was used as the source of $Cu_{K\alpha}$ radiation ($\lambda = 0.154$ nm). Monochromatization of the primary beam was achieved by using a curved Ge crystal. Scattered radiation was measured by using a Nonius CPS120 position-sensitive detector. The resolution of this detector in 2θ was 0.018°.

[1] J. M. Lehn, *Polym. Int.* **2002**, *51*, 825; U. S. Schubert, C. Eschbaumer, *Angew. Chem.* **2002**, *114*, 3016; U. S. Schubert, C. Eschbaumer, *Angew. Chem. Int. Ed.* **2002**, *41*, 2892; L. Brunsveld, B. J. B. Folmer, E. W. Meijer, R. P. Sijbesma, *Chem. Rev.* **2001**, *101*, 4071.

[2] D. C. Sherrington, K. A. Taskinen, *Chem. Soc. Rev.* **2001**, *30*, 83; J. M. Lehn, M. Masscal, A. Decian, F. Fischer, *J. Chem. Soc. Perkin Trans. 1* **1992**, 461; T. Kato, N. Mizoshita, K. Kanie, *Macromol. Rapid Commun.* **2001**, *22*, 797; M. Shirakawa, N. Fujita, S. Seiji, *J. Am. Chem. Soc.* **2003**, *125*, 9902.

[3] R. Dobrawa, F. Wurthner, *Chem. Commun.* **2002**, 1878; F. T. Edelmann, I. Haiduc, *Supramolecular Organometallic Chemistry*, Wiley-VCH, Weinheim, **1999**; B. G. G. Lohmeijer, U. S. Schubert, *Angew. Chem.* **2002**, *114*, 3980; B. G. G. Lohmeijer, U. S. Schubert, *Angew. Chem. Int. Ed.* **2002**, *41*, 3825.

[4] H. Engelkamp, S. Middelbeek, R. J. M. Nolte, *Science* **1999**, *284*, 785; *Handbook of Liquid Crystals, Vol. 2B* (Eds.: D. Demus, J. Goodby, G. W. Gray, H. W. Spiess, V. Vill), Wiley-VCH, Weinheim, **1998**.

[5] G. Gottarellin, G. P. Spada, A. Garbesi, *Comprehensive Supramolecular Chemistry, Vol. 9* (Ed.: J. M. Lehn), Pergamon Press, Oxford, **1996**, pp. 483.

[6] C. F. J. Faul, M. Antonietti, *Adv. Mater.* **2003**, *15*, 673.

[7] Y. Guan, M. Antonietti, C. F. J. Faul, *Langmuir* **2002**, *18*, 5939; C. F. J. Faul, M. Antonietti, *Chem. Eur. J.* **2002**, *8*, 2764; F. Camerel, M. Antonietti, C. F. J. Faul, *Chem. Eur. J.* **2003**, *9*, 2160.

[8] Y. Guan, Y. Zakrevskyy, J. Stumpe, M. Antonietti, C. F. J. Faul, *Chem. Commun.* **2003**, 894.

[9] B. A. Gregg, R. A. Cormier, *J. Phys. Chem. B* **1998**, *102*, 9952; R. Bonnett, *Chem. Soc. Rev.* **1995**, *24*, 19.

[10] T. Boom, R. T. Hayes, Y. Zhao, P. J. Bushard, E. A. Weiss, M. R. Wasielewski, *J. Am. Chem. Soc.* **2002**, *124*, 9582; R. S. Loewe, K. Tomizake, W. J. Youngblood, Z. Bo, J. S. Lindsey, *J. Mater. Chem.* **2002**, *12*, 3438.

[11] M. A. Miller, R. K. Lammi, S. Prathapan, D. Holten, J. S. Lindsey, *J. Org. Chem.* **2000**, *65*, 6634.

[12] D. M. Adams, J. Kerimo, E. J. C. Olson, A. Zaban, B. A. Gregg, P. F. Barbara, *J. Am. Chem. Soc.* **1997**, *119*, 10608.

[13] C. W. Tang, *Appl. Phys. Lett.* **1986**, *48*, 183; J. Rotalski, D. Meissner, *Solar Energy Materials and Solar Cells* **2000**, *63*, 37; M. Thelakkat, C. Schmitz, H. W. Schmidt, *Adv. Mater.* **2002**, *14*, 577.

[14] T. Vermonden, J. Ven der Gucht, P. Waard, A. T. M. Marcelis, N. A. M. Besseling, E. J. R. Sudholter, G. J. Fleer, M. A. C. Stuart, *Macromolecules* **2003**, *36*, 7035.

[15] R. B. Martin, *Chem. Rev.* **1996**, *96*, 3043; F. Wuerthner, C. Thalacker, S. Diele, C Tschierske, *Chem. Eur. J.* **2001**, *7*, 2245.

[16] P. Terech, R. G. Weiss, *Chem. Rev.* **1997**, *97*, 3133; R. H. Wade, P. Terech, E. A. Hewat, R. Ramasseul, F. Volino, *J. Colloid Interface Sci.* **1986**, *114*, 442.

[17] H. von Berlepsch, C. Böttcher, *J. Phys. Chem. B* **2002**, *106*, 3146.

[18] M. M. Golas, B. Sander, C. L. Will, R. Luhrmann, H. Stark, *Science* **2003**, *300*, 980.

[19] K. Ludwig, B. Baljinnyam, A. Herrmann, C. Böttcher, *Embo J.* **2003**, *22*, 3761.

[20] C. Böttcher, H. Stark, M. van Heel, *Ultramicroscopy* **1996**, 133.

[21] M. Kellermann, W. Bauer, A. Hirsch, B. Schade, K. Ludwig, C. Böttcher, *Angew. Chem.* **2004**, *116*, 3019; *Angew. Chem. Int. Ed.* **2004**, *43*, 2959.

[22] S. H. Yu, H. Colfen, M. Antonietti, *Chem. Eur. J.* **2002**, *8*, 2937.

[23] H. Schnablegger, M. Antonietti, C. Goltner, I. H. Stapff, F. Brink-Spalink, A. Greiner, *Acta Polymerica* **1999**, *50*, 391.

[24] a) S. G. Liu, G. Sui, R. A. Cormier, R. M. Leblanc, B. A. Gregg, *J. Phys. Chem. B* **2002**, *106*, 1307; b) Y. Liu, S. Lei, S. Yin, S. Xu, Q. Zheng, Q. Zeng, C. Wang, L. Wan, C. Bai, *J. Phys. Chem. B* **2002**, *106*, 12569.

[25] M. van Heel, G. Harauz, E. V. Orlova, R. Schmidt, M. Schatz, *J. Struct. Biol.* **1996**, *116*, 17.